

Energy Stable Boundary Conditions for the Nonlinear Incompressible Navier-Stokes Equations

Jan Nordström and Cristina La Cognata

The self-archived postprint version of this journal article is available at Linköping University Institutional Repository (DiVA):

<http://urn.kb.se/resolve?urn=urn:nbn:se:liu:diva-153296>

N.B.: When citing this work, cite the original publication.

Nordström, J., La Cognata, C., (2019), Energy Stable Boundary Conditions for the Nonlinear Incompressible Navier-Stokes Equations, *Mathematics of Computation*, 88(316), 665-690.
<https://doi.org/10.1090/mcom/3375>

Original publication available at:

<https://doi.org/10.1090/mcom/3375>

Copyright: American Mathematical Society

<http://www.ams.org/journals/>



ENERGY STABLE BOUNDARY CONDITIONS FOR THE NONLINEAR INCOMPRESSIBLE NAVIER-STOKES EQUATIONS

JAN NORDSTRÖM AND CRISTINA LA COGNATA

ABSTRACT. The nonlinear incompressible Navier-Stokes equations with different types of boundary conditions at far fields and solid walls is considered. Two different formulations of boundary conditions are derived using the energy method. Both formulations are implemented in both strong and weak form and lead to an estimate of the velocity field.

Equipped with energy bounding boundary conditions, the problem is approximated by using discrete derivative operators on summation-by-parts form and weak boundary and initial conditions. By mimicking the continuous analysis, the resulting semi-discrete as well as fully discrete scheme are shown to be provably stable, divergence free and high-order accurate.

1. INTRODUCTION

The nonlinear incompressible Navier-Stokes equations are regularly used in models of climate and weather forecasts, ocean circulation predictions [30, 46, 54], studies of turbulent airflow around vehicles [21, 26], studies of blood flow [12, 53], analysis of pollution [17, 43] and many others fields. Various formulations of the incompressible Navier-Stokes model have been proposed. The velocity-pressure formulation, where the explicit divergence relation is omitted, is the most common choice. Popular numerical techniques to enforce zero divergence for this form include staggered grids [16, 28] and projections or fractional step methods [49, 25]. Yet another procedure is to modify the pressure equation [18, 44] or devise boundary conditions [24, 39] which systematically damp the divergence inside the computational domain.

In this paper we consider the Navier-Stokes equations in the original velocity-divergence form directly, which bypasses the need for the special divergence reducing techniques mentioned above. The boundary conditions are derived in a form that is similar to the characteristic boundary conditions for hyperbolic problems (and generalized to the compressible Navier-Stokes equations in [32, 42]). We follow the general procedure for initial boundary value problems (IBVP) outlined in [34] and define outgoing and ingoing variables at the boundaries. The latter are specified in terms of the former and data in order to get an energy estimate.

Two formulations stemming from two different techniques to diagonalize the boundary terms are presented. In the first formulation, the boundary conditions

Received by the editor April 23, 2018.

2010 *Mathematics Subject Classification.* Primary 65M12, 65M06, 35M33, 76D05.

Key words and phrases. Navier-Stokes equations, incompressible, boundary conditions, energy estimate, stability, summation-by-parts, high-order accuracy, divergence free.

are obtained through a non-singular rotation while, in the second formulation, they are derived directly by an eigenvalue decomposition. Both formulations are strongly and weakly imposed and we observe that they naturally come in nonlinear form. We derive general boundary conditions, but pay particular attention to solid wall and Dirichlet conditions for the velocities as well as natural and stabilized natural boundary conditions. Furthermore, it is shown that it is not necessary to provide pressure data in the initial and boundary conditions, to obtain the full solution.

The nonlinear system is discretized in space and time by using discrete derivative operators on Summation-By-Parts (SBP) form [52, 48, 31] and the boundary and initial conditions are weakly imposed with the Simultaneous-Approximation-Term (SAT) technique [7, 50]. The resulting SBP-SAT approximation is proved to be stable in both a semi-discrete and fully discrete sense. The discrete derivation is for simplicity and ease of presentation done for SBP-SAT schemes on tensor product form. Examples of such schemes include finite difference [50, 51, 37], spectral element [6, 5] and discontinuous Galerkin schemes [19, 13, 55]. The derivation is also valid for genuinely multi-dimensional SBP-SAT schemes [9, 56] as well as finite volume [36, 35] and flux reconstruction schemes [23, 8, 45] on SBP-SAT form.

The paper proceeds as follows. In Section 2, we introduce and discuss the continuous problem and derive boundary conditions. Next, in Section 3, the general form of boundary conditions are related to a few commonly used ones. It is also shown how to impose the boundary condition without involving the pressure. A comparison discussing the advantages and disadvantages of the two formulations is provided in Section 4. In Section 5, the semi-discrete version of the governing equations and the SAT terms for the boundary conditions are derived, and stability is proven. The fully discrete SBP-SAT approximation and a complete stability analysis is presented in Section 6. Conclusions are drawn in Section 7.

2. THE CONTINUOUS PROBLEM

Consider the incompressible Navier-Stokes equations with velocity field $\mathbf{u} = (u, v)$, pressure p and viscosity ϵ

$$(2.1) \quad \begin{aligned} u_t + uu_x + vv_y + p_x - \epsilon(u_{xx} + u_{yy}) &= 0, \\ v_t + uv_x + vv_y + p_y - \epsilon(v_{xx} + v_{yy}) &= 0, \\ u_x + v_y &= 0. \end{aligned}$$

By letting $\mathbf{v} = (u, v, p)^T$ and introducing the matrices

$$(2.2) \quad A = \begin{bmatrix} u & 0 & 1 \\ 0 & u & 0 \\ 1 & 0 & 0 \end{bmatrix}, \quad B = \begin{bmatrix} v & 0 & 0 \\ 0 & v & 1 \\ 0 & 1 & 0 \end{bmatrix} \quad \text{and} \quad \tilde{I} = \begin{bmatrix} 1 & 0 & 0 \\ 0 & 1 & 0 \\ 0 & 0 & 0 \end{bmatrix},$$

the system (2.1) can be written as

$$(2.3) \quad \tilde{I}\mathbf{v}_t + A\mathbf{v}_x + B\mathbf{v}_y - \epsilon\tilde{I}(\mathbf{v}_{xx} + \mathbf{v}_{yy}) = 0.$$

Next, we rewrite the convection terms in (2.1) as

$$(2.4) \quad A\mathbf{v}_x = \frac{1}{2}(A\mathbf{v})_x + \frac{1}{2}A\mathbf{v}_x - \frac{1}{2}A_x\mathbf{v}, \quad B\mathbf{v}_y = \frac{1}{2}(B\mathbf{v})_y + \frac{1}{2}B\mathbf{v}_y - \frac{1}{2}B_y\mathbf{v}.$$

By inserting (2.4) into (2.3) and recalling that we are dealing with an incompressible fluid, i.e., $A_x + B_y = (u_x + v_y)\tilde{I} = 0$, we obtain the initial boundary value problem

for the *skew-symmetric* form of the incompressible Navier-Stokes equations

$$(2.5) \quad \tilde{I}\mathbf{v}_t + \frac{1}{2}[(A\mathbf{v})_x + A\mathbf{v}_x + (B\mathbf{v})_y + B\mathbf{v}_y] - \epsilon\tilde{I}\Delta\mathbf{v} = 0, \quad (x, y) \in \Omega, t > 0$$

$$(2.6) \quad H\mathbf{v} = \mathbf{g}, \quad (x, y) \in \partial\Omega, t > 0$$

$$(2.7) \quad \mathbf{v} = \mathbf{f}, \quad (x, y) \in \Omega, t = 0.$$

In (2.6)-(2.7), \mathbf{g} and \mathbf{f} are the initial and boundary data, respectively. The boundary operator H will be specified on $\partial\Omega$ such that the correct (minimal) number and type of boundary conditions are imposed.

Remark 2.1. The nonlinear terms must be split into skew-symmetric form for the upcoming discrete analysis. For more details regarding different splitting techniques, see [33, 11, 47]. Note that the systems (2.3) and (2.5) are symmetric which allows for a straightforward use of the energy method.

Remark 2.2. Existence requires that (2.6) constitutes a minimal set of boundary conditions. This means that the correct (minimal) number of linearly independent rows in H must be imposed. Too few boundary conditions will neither lead to an estimate nor uniqueness.

Remark 2.3. We consider smooth compatible data and, consequently, smooth solutions for the problem (2.5)-(2.7). Normally, nonlinear well-posedness would follow as an extension of linear well-posedness through the linearization and localisation principles, see [27]. However, no explicit bound on the pressure is derived in this paper, hence we do not refer to the resulting formulation as well-posed.

2.1. The energy estimate. The energy method and Green's theorem applied to (2.5) yield

$$(2.8) \quad \frac{d}{dt}\|\mathbf{v}\|_{\tilde{I}}^2 + 2\epsilon\|\nabla\mathbf{v}\|_{\tilde{I}}^2 = \text{BT},$$

where $\|\mathbf{v}\|_{\tilde{I}}^2 = \int_{\Omega} \mathbf{v}^T \tilde{I} \mathbf{v}$ is a semi-norm that allows for $\|\mathbf{v}\|_{\tilde{I}} = 0$ even for $p \neq 0$. In (2.8), BT denotes the boundary term

$$(2.9) \quad \text{BT} = - \oint_{\Omega} \mathbf{v}^T (An_x + Bn_y) \mathbf{v} - 2\epsilon \mathbf{v}^T \tilde{I} [\mathbf{v}_x n_x + \mathbf{v}_y n_y] ds,$$

where $ds = \sqrt{dx^2 + dy^2}$ and $\mathbf{n} = (n_x, n_y)$ is the outward pointing unit normal vector on $\partial\Omega$. To derive an estimate based on (2.8), we must bound BT.

We start by introducing a change of variables

$$(2.10) \quad \mathbf{w} = \begin{bmatrix} u_n \\ u_s \\ p \\ \epsilon \partial_{\mathbf{n}} u_n \\ \epsilon \partial_{\mathbf{n}} u_s \end{bmatrix} = T \mathbf{v}, \quad T = \begin{bmatrix} n_x & n_y & 0 \\ -n_y & n_x & 0 \\ 0 & 0 & 1 \\ \epsilon \partial_{\mathbf{n}} n_x & \epsilon \partial_{\mathbf{n}} n_y & 0 \\ -\epsilon \partial_{\mathbf{n}} n_y & \epsilon \partial_{\mathbf{n}} n_x & 0 \end{bmatrix},$$

where u_n and u_s denote the outward normal and tangential velocity components, respectively, and $\partial_{\mathbf{n}} = \mathbf{n} \cdot \nabla = n_x \partial_x + n_y \partial_y$ is the normal derivative. Next, we

apply (2.10) to (2.9) and rearrange such that BT becomes

$$(2.11) \quad \text{BT} = - \oint_{\Omega} \begin{bmatrix} u_n \\ u_s \\ p \\ \epsilon \partial_{\mathbf{n}} u_n \\ \epsilon \partial_{\mathbf{n}} u_s \end{bmatrix}^T \underbrace{\begin{bmatrix} u_n & 0 & 1 & -1 & 0 \\ 0 & u_n & 0 & 0 & -1 \\ 1 & 0 & 0 & 0 & 0 \\ -1 & 0 & 0 & 0 & 0 \\ 0 & -1 & 0 & 0 & 0 \end{bmatrix}}_{A_{\mathbf{n}}} \begin{bmatrix} u_n \\ u_s \\ p \\ \epsilon \partial_{\mathbf{n}} u_n \\ \epsilon \partial_{\mathbf{n}} u_s \end{bmatrix} ds.$$

We need a minimal number of boundary conditions such that $\mathbf{w}^T A_{\mathbf{n}} \mathbf{w} \geq 0$.

Remark 2.4. Note that the boundary matrix $A_{\mathbf{n}}$ in (2.11) depend on the normal velocity u_n . This dependence will be discussed in the up-coming analysis of the form of the boundary conditions and will be investigated in the critical case when $u_n \rightarrow 0$.

2.2. Boundary conditions. We follow the roadmap in [34] for IBVP's and focus on the items:

- (1) *The number of boundary conditions.* The boundary term (2.11) will be diagonalized using different techniques. The minimal number of boundary conditions is equal to the number of negative diagonal entries.
- (2) *The form of the boundary conditions.* The transformed variables associated to the negative diagonal elements (ingoing variables) are specified in terms of the ones corresponding to positive diagonal elements (outgoing variables) and boundary data.
- (3) *The strong implementation.* The boundary conditions are chosen such that a negative semi-definite boundary term is obtained for zero boundary data.
- (4) *The weak implementation.* The weak imposition of the new boundary conditions is chosen such that it leads to the same estimate as the strong imposition augmented with a dissipative boundary term.

2.2.1. The number of boundary conditions using rotations. A symmetric matrix A can be diagonalized by a suitable non-singular rotation matrix M . The elements of the resulting diagonal matrix, $\Lambda = M^T A M$, are not necessarily the eigenvalues of A , but the number of positive and negative diagonal entries is the same. For more details regarding diagonalizations with rotations see [42, 34].

A complete diagonalization of the boundary matrix $A_{\mathbf{n}}$ in (2.11) is given by

$$(2.12) \quad \Lambda_M = M^T A_{\mathbf{n}} M, \quad \text{with rotation} \quad M = \begin{bmatrix} u_n & 0 & 1 & -1 & 0 \\ 0 & u_n & 0 & 0 & -1 \\ 0 & 0 & 0 & 1 & 0 \\ 0 & 0 & 1 & -1 & 0 \\ 0 & 0 & 0 & 0 & 1 \end{bmatrix}^{-1}.$$

The diagonal matrix and vector of linearly independent rotated variables are

$$(2.13) \quad \Lambda_M = \frac{1}{u_n} \begin{bmatrix} 1 & 0 & 0 & 0 & 0 \\ 0 & 1 & 0 & 0 & 0 \\ 0 & 0 & 0 & 0 & 0 \\ 0 & 0 & 0 & -1 & 0 \\ 0 & 0 & 0 & 0 & -1 \end{bmatrix} \quad \text{and} \quad \mathbf{W} = M^{-1} \mathbf{w} = \begin{bmatrix} u_n^2 + p - \epsilon \partial_{\mathbf{n}} u_n \\ u_n u_s - \epsilon \partial_{\mathbf{n}} u_s \\ \epsilon \partial_{\mathbf{n}} u_n \\ p - \epsilon \partial_{\mathbf{n}} u_n \\ \epsilon \partial_{\mathbf{n}} u_s \end{bmatrix}.$$

Note that, the matrix Λ_M in (2.13) always has two positive and two negative diagonal entries. Consequently, the problem (2.5) requires two boundary conditions both at an inflow boundary ($u_n < 0$) and an outflow boundary ($u_n > 0$).

Next, we write $\Lambda_M = \text{diag}(\Lambda^+, 0, \Lambda^-)$, where Λ^- and Λ^+ contain the negative and positive diagonal elements, and indicate with W^- and W^+ the corresponding variables. In the inflow case we have

$$(2.14) \quad W^- = \begin{bmatrix} u_n^2 + p - \epsilon \partial_{\mathbf{n}} u_n \\ u_n u_s - \epsilon \partial_{\mathbf{n}} u_s \end{bmatrix}, W^+ = \begin{bmatrix} p - \epsilon \partial_{\mathbf{n}} u_n \\ \epsilon \partial_{\mathbf{n}} u_s \end{bmatrix}, \Lambda^- = \frac{1}{u_n} I_2, \Lambda^+ = -\Lambda^-,$$

while in the outflow case, the signs are flipped and we have

$$(2.15) \quad W^- = \begin{bmatrix} p - \epsilon \partial_{\mathbf{n}} u_n \\ \epsilon \partial_{\mathbf{n}} u_s \end{bmatrix}, W^+ = \begin{bmatrix} u_n^2 + p - \epsilon \partial_{\mathbf{n}} u_n \\ u_n u_s - \epsilon \partial_{\mathbf{n}} u_s \end{bmatrix}, \Lambda^- = -\frac{1}{u_n} I_2, \Lambda^+ = -\Lambda^-.$$

In both situations, the variable corresponding to the zero eigenvalue is $W^0 = \epsilon \partial_{\mathbf{n}} u_n$, while W^- and W^+ are called the in- and outgoing *rotated variables*, respectively. With this notation, the quadratic form in (2.11) can be written

$$(2.16) \quad \text{BT} = - \oint \begin{bmatrix} W^+ \\ W^- \end{bmatrix}^T \begin{bmatrix} \Lambda^+ & 0 \\ 0 & \Lambda^- \end{bmatrix} \begin{bmatrix} W^+ \\ W^- \end{bmatrix},$$

where the variable corresponding to the zero diagonal entry is ignored.

2.2.2. The number of boundary conditions using eigenvalues. The correct number of boundary conditions can also be obtained by directly finding the eigenvalues of $A_{\mathbf{n}}$ in (2.11), see also [40, 39]. The eigenvalue problem $|A_{\mathbf{n}} - \lambda I_5| = 0$ defines a characteristic polynomial equation with five distinct real roots $\lambda_1 < \lambda_2 < \lambda_3 < \lambda_4 < \lambda_5$ and eigenvalue matrix $\Lambda = \text{diag}(\lambda_1, \dots, \lambda_5)$, where

$$(2.17) \quad \lambda_{1,5} = \frac{u_n}{2} \mp \sqrt{\left(\frac{u_n}{2}\right)^2 + 2}, \quad \lambda_3 = 0, \quad \lambda_{2,4} = \frac{u_n}{2} \mp \sqrt{\left(\frac{u_n}{2}\right)^2 + 1}.$$

The associated orthonormal basis of eigenvectors is indicated by $\bar{X} = XN$ and it leads to the eigenvalue decomposition

$$(2.18) \quad A_{\mathbf{n}} = \bar{X} \Lambda \bar{X}^T = X N \Lambda (X N)^T, \quad \text{where} \quad X = - \begin{bmatrix} \lambda_1 & 0 & 0 & 0 & \lambda_5 \\ 0 & \lambda_2 & 0 & \lambda_4 & 0 \\ 1 & 0 & -1 & 0 & 1 \\ -1 & 0 & -1 & 0 & -1 \\ 0 & -1 & 0 & -1 & 0 \end{bmatrix}$$

and $N^{-1} = \text{diag}(\sqrt{2 + \lambda_1^2}, \sqrt{1 + \lambda_2^2}, \sqrt{2}, \sqrt{1 + \lambda_3^2}, \sqrt{2 + \lambda_5^2})$ contains the normalizing weights of the columns in X .

The diagonal matrix and linearly independent characteristic variables are

$$(2.19) \quad \Lambda_X = N \Lambda N^T \quad \text{and} \quad \mathbf{W} = X^T \mathbf{w} = \begin{bmatrix} \lambda_1 u_n + p - \epsilon \partial_{\mathbf{n}} u_n \\ \lambda_2 u_s - \epsilon \partial_{\mathbf{n}} u_s \\ p + \epsilon \partial_{\mathbf{n}} u_n \\ \lambda_4 u_s - \epsilon \partial_{\mathbf{n}} u_s \\ \lambda_5 u_n + p - \epsilon \partial_{\mathbf{n}} u_n \end{bmatrix}$$

respectively. Next, we introduce $W^+ = (X^T \mathbf{w})^+$ and $W^- = (X^T \mathbf{w})^-$ given by

$$(2.20) \quad W^- = \begin{bmatrix} \lambda_1 u_n + p - \epsilon \partial_{\mathbf{n}} u_n \\ \lambda_2 u_s - \epsilon \partial_{\mathbf{n}} u_s \end{bmatrix}, \quad W^+ = \begin{bmatrix} \lambda_4 u_s - \epsilon \partial_{\mathbf{n}} u_s \\ \lambda_5 u_n + p - \epsilon \partial_{\mathbf{n}} u_n \end{bmatrix}.$$

With a slight abuse of notation, we denote by W^- and W^+ the in- and outgoing *characteristic variables*, respectively. The variable corresponding to the zero eigenvalue is $W^0 = p + \epsilon \partial_{\mathbf{n}} u_n$.

Note that $\lambda_1, \lambda_2 < 0$ and $\lambda_4, \lambda_5 > 0$ for all values of u_n . This implies that (as in the previous case) we need two boundary conditions. Moreover, given (2.20) and the diagonal matrices

$$(2.21) \quad \Lambda^- = \begin{bmatrix} \lambda_1/(2 + \lambda_1^2) & 0 \\ 0 & \lambda_2/(1 + \lambda_2^2) \end{bmatrix}, \quad \Lambda^+ = \begin{bmatrix} \lambda_4/(1 + \lambda_4^2) & 0 \\ 0 & \lambda_5/(2 + \lambda_5^2) \end{bmatrix}$$

we can again rewrite BT in (2.11) in the diagonal form (2.16).

Remark 2.5. The number of boundary conditions is independent of the specific transformation used to arrive at the diagonal form (2.16), as long as the resulting variables are linearly independent. This follows from Sylvester's law of inertia, see [42, 22] for details. The two specific transformations presented above (there might be even more) lead to different forms of boundary conditions, which is the next topic.

2.2.3. The form of the boundary conditions. We start by considering the most general form of boundary conditions

$$W^- - RW^+ - R^0 W^0 = \mathbf{g},$$

where R and R^0 are 2-by-2 and 2-by-1 coefficient matrices, respectively, and $\mathbf{g} = (g_1, g_2)^T$ contains the boundary data. The first result is

Proposition 2.6. The form of boundary condition that bounds (2.16) cannot involve the variable corresponding to the zero eigenvalue.

Proof. Consider the homogeneous case of the form $W^- = RW^+ + R^0 W^0$ and insert it in (2.16). We find

$$\text{BT} = - \oint_{\Omega} \begin{bmatrix} W^+ \\ W^0 \end{bmatrix}^T \begin{bmatrix} \Lambda^+ + R^T \Lambda^- R & R^T \Lambda^- R^0 \\ (R^0)^T \Lambda^- R & (R^0)^T \Lambda^- R^0 \end{bmatrix} \begin{bmatrix} W^+ \\ W^0 \end{bmatrix} ds,$$

which directly implies that R^0 must be identical to zero. \square

The general form of boundary conditions that bounds the right-hand side in (2.16) (as well as in (2.9)) is hence given by

$$(2.22) \quad H\mathbf{v} = W^- - RW^+ = \mathbf{g},$$

where R is a 2-by-2 matrix and $\mathbf{g} = (g_1, g_2)^T$ contains the boundary data. This is a nonlinear version of the result in [34] for a linear IBVPs.

The formulation (2.22) decomposes the boundary operator H into

$$(2.23) \quad H\mathbf{v} = (H^- - RH^+)\mathbf{v}.$$

In the rotated formulation, H^+ and H^- are given by

$$(2.24) \quad H^+ \mathbf{v} = (M^{-1})^+ T \mathbf{v} = W^+, \quad H^- \mathbf{v} = (M^{-1})^- T \mathbf{v} = W^-,$$

with M^{-1} from (2.12) and T from (2.10). In particular, for the inflow case

$$(2.25) \quad (M^{-1})^+ = \begin{bmatrix} u_n & 0 & 1 & -1 & 0 \\ 0 & u_n & 0 & 0 & -1 \end{bmatrix}, \quad (M^{-1})^- = \begin{bmatrix} 0 & 0 & 1 & -1 & 0 \\ 0 & 0 & 0 & 0 & 1 \end{bmatrix}$$

while in outflow case they are interchanged.

In a similar way, the characteristic variable formulation gives

$$(2.26) \quad H^+ \mathbf{v} = (X^T)^+ T \mathbf{v} = W^+, \quad H^- \mathbf{v} = (X^T)^- T \mathbf{v} = W^-,$$

with X from (2.18) and

$$(2.27) \quad (X^T)^- = \begin{bmatrix} \lambda_1 & 0 & 1 & -1 & 0 \\ 0 & \lambda_2 & 0 & 0 & -1 \end{bmatrix}, \quad (X^T)^+ = \begin{bmatrix} 0 & \lambda_4 & 0 & 0 & -1 \\ \lambda_5 & 0 & 1 & -1 & 0 \end{bmatrix}.$$

Remark 2.7. The boundary conditions in (2.22)-(2.27) are in general nonlinear.

2.3. The implementation procedure. We start with the strong form of the boundary procedure.

2.3.1. The strong implementation. The following proposition is a nonlinear version of the linear result in [34].

Proposition 2.8. The boundary conditions (2.22) bounds (2.16) if

$$(2.28) \quad \Lambda^+ + R^T \Lambda^- R > 0$$

and a positive semi-definite or positive definite matrix Γ exists such that

$$(2.29) \quad -\Lambda^- + (\Lambda^- R)[\Lambda^+ + R^T \Lambda^- R]^{-1}(\Lambda^- R)^T \leq \Gamma < \infty.$$

Proof. Consider condition (2.22) and replace W^- with $RW^+ + \mathbf{g}$ in (2.16) to get

$$(2.30) \quad \text{BT} = - \oint_{\Omega} \begin{bmatrix} W^+ \\ \mathbf{g} \end{bmatrix}^T \begin{bmatrix} \Lambda^+ + R^T \Lambda^- R & R^T \Lambda^- \\ \Lambda^- R & \Lambda^- \end{bmatrix} \begin{bmatrix} W^+ \\ \mathbf{g} \end{bmatrix} ds.$$

By adding and subtracting $\oint_{\Omega} \mathbf{g}^T \Gamma \mathbf{g} ds$ to (2.30), where Γ is a positive semi-definite or positive definite matrix, we find

$$(2.31) \quad \text{BT} = - \oint_{\Omega} \begin{bmatrix} W^+ \\ \mathbf{g} \end{bmatrix}^T \begin{bmatrix} \Lambda^+ + R^T \Lambda^- R & R^T \Lambda^- \\ \Lambda^- R & \Gamma + \Lambda^- \end{bmatrix} \begin{bmatrix} W^+ \\ \mathbf{g} \end{bmatrix} ds + \oint_{\Omega} \mathbf{g}^T \Gamma \mathbf{g} ds.$$

Now consider the following matrix decomposition

$$\begin{bmatrix} \Lambda^+ + R^T \Lambda^- R & R^T \Lambda^- \\ \Lambda^- R & \Gamma + \Lambda^- \end{bmatrix} = Y^T M Y, \quad Y = \begin{bmatrix} I & Z \\ 0 & I \end{bmatrix},$$

where $Z = [\Lambda^+ + R^T \Lambda^- R]^{-1} R^T$ and

$$(2.32) \quad M = \begin{bmatrix} \Lambda^+ + R^T \Lambda^- R & 0 \\ 0 & \Gamma + \Lambda^- - (\Lambda^- R)[\Lambda^+ + R^T \Lambda^- R]^{-1}(\Lambda^- R)^T \end{bmatrix}.$$

If (2.28) holds and we choose Γ such that the lower bound in (2.29) holds, it follows that the matrix M in (2.32) is positive semi-definite and (2.31) becomes

$$(2.33) \quad \text{BT} = - \oint_{\Omega} \begin{bmatrix} W^+ \\ \mathbf{g} \end{bmatrix}^T Y^T M Y \begin{bmatrix} W^+ \\ \mathbf{g} \end{bmatrix} ds + \oint_{\Omega} \mathbf{g}^T \Gamma \mathbf{g} ds \leq \oint_{\Omega} \mathbf{g}^T \Gamma \mathbf{g} ds.$$

If in addition, also the upper bound in (2.29) holds, we have an estimate. \square

Remark 2.9. In the linear case studied in [34], condition (2.28) suffices.

Corollary 2.10. The homogeneous boundary conditions $W^- = RW^+$ leads to a bound for (2.16) if

$$(2.34) \quad \Lambda^+ + R^T \Lambda^- R \geq 0.$$

Proof. Consider (2.22) with $\mathbf{g} = 0$. The boundary term (2.30) becomes

$$(2.35) \quad \text{BT} = - \oint_{\Omega} W^{+T} [\Lambda^+ + R^T \Lambda^- R] W^+ ds \leq 0.$$

□

2.3.2. The weak implementation. The boundary conditions (2.22) can also be weakly imposed by adding the penalty term $L(\Sigma(W^- - RW^+ - \mathbf{g}))$ to the right-hand side of (2.5) yielding

$$(2.36) \quad \tilde{I}\mathbf{v}_t + \frac{1}{2}[(A\mathbf{v})_x + A\mathbf{v}_x + (B\mathbf{v})_y + B\mathbf{v}_y] - \epsilon \tilde{I}\Delta\mathbf{v} = L(\Sigma(W^- - RW^+ - \mathbf{g})).$$

Here, L is a lifting operator [1] defined such that, for smooth vector functions ϕ, ψ

$$\int_{\Omega} \phi^T L(\psi) dx dy = \oint_{\partial\Omega} \phi^T \psi ds,$$

holds. In (2.36), Σ is a penalty matrix to be determined.

Proposition 2.11. The weak imposition of the boundary conditions in (2.36) with

$$(2.37) \quad \Sigma = (H^-)^T \Lambda^-$$

leads to a bound on the energy if (2.28) and (2.29) holds.

Proof. The energy method applied to (2.36) leads to (2.8) with two additional boundary terms

$$(2.38) \quad \begin{aligned} \text{BT} = & - \oint_{\partial\Omega} \begin{bmatrix} W^+ \\ W^- \end{bmatrix}^T \begin{bmatrix} \Lambda^+ & 0 \\ 0 & \Lambda^- \end{bmatrix} \begin{bmatrix} W^+ \\ W^- \end{bmatrix} ds \\ & + \oint_{\partial\Omega} \mathbf{v}^T \Sigma (W^- - RW^+ - \mathbf{g}) + [\mathbf{v}^T \Sigma (W^- - RW^+ - \mathbf{g})]^T ds. \end{aligned}$$

The introduction of Σ in (2.37) such that $\mathbf{v}^T \Sigma = (W^-)^T \Lambda^-$ leads to

$$(2.39) \quad \text{BT} = - \oint_{\partial\Omega} \begin{bmatrix} W^+ \\ W^- \\ \mathbf{g} \end{bmatrix}^T \begin{bmatrix} \Lambda^+ & R^T \Lambda^- & 0 \\ \Lambda^- R & -\Lambda^- & \Lambda^- \\ 0 & \Lambda^- & 0 \end{bmatrix} \begin{bmatrix} W^+ \\ W^- \\ \mathbf{g} \end{bmatrix} ds.$$

The splitting

$$(2.40) \quad \begin{bmatrix} \Lambda^+ & R^T \Lambda^- & 0 \\ \Lambda^- R & -\Lambda^- & \Lambda^- \\ 0 & \Lambda^- & 0 \end{bmatrix} = \begin{bmatrix} -R^T \Lambda^- R & R^T \Lambda^- & -R^T \Lambda^- \\ \Lambda^- R & -\Lambda^- & \Lambda^- \\ -\Lambda^- R & \Lambda^- & -\Lambda^- \end{bmatrix} + \begin{bmatrix} \Lambda^+ + R^T \Lambda^- R & 0 & R^T \Lambda^- \\ 0 & 0 & 0 \\ \Lambda^- R & 0 & \Gamma + \Lambda^- \end{bmatrix} - \begin{bmatrix} 0 & 0 & 0 \\ 0 & 0 & 0 \\ 0 & 0 & \Gamma \end{bmatrix}$$

transforms (2.39) to

$$(2.41) \quad \begin{aligned} \text{BT} = & \oint_{\partial\Omega} (W^- - RW^+ - \mathbf{g})^T \Lambda^- (W^- - RW^+ - \mathbf{g}) ds \\ & - \oint_{\Omega} \begin{bmatrix} W^+ \\ \mathbf{g} \end{bmatrix}^T \begin{bmatrix} \Lambda^+ + R^T \Lambda^- R & R^T \Lambda^- \\ \Lambda^- R & \Gamma + \Lambda^- \end{bmatrix} \begin{bmatrix} W^+ \\ \mathbf{g} \end{bmatrix} ds + \oint_{\Omega} \mathbf{g}^T \Gamma \mathbf{g} ds. \end{aligned}$$

Clearly, the first term on the right-hand side of (2.41) is non-positive. The other two are identical to the ones in (2.31) obtained with the strong imposition and lead to (2.33). \square

Corollary 2.12. The weak imposition of the homogeneous boundary condition in (2.36) together with (2.37) leads to a bound on the energy if (2.34) holds.

Proof. Consider the homogeneous version of (2.36), i.e., with data $\mathbf{g} = 0$ and Σ as in (2.37). The same procedure as in the proof of Proposition 2.11 leads to

$$\text{BT} = - \oint_{\partial\Omega} \begin{bmatrix} W^+ \\ W^- \end{bmatrix}^T \begin{bmatrix} \Lambda^+ & R^T \Lambda^- \\ \Lambda^- R & -\Lambda^- \end{bmatrix} \begin{bmatrix} W^+ \\ W^- \end{bmatrix} ds.$$

By adding and subtracting $\oint (W^+)^T [R^T \Lambda^- R] W^+ ds$, we find

$$\text{BT} = - \oint_{\partial\Omega} (W^+)^T [\Lambda^+ + R^T \Lambda^- R] W^+ + \oint_{\partial\Omega} [W^- - RW^+]^T \Lambda^- [W^- - RW^+]$$

which is non-positive if (2.34) holds. \square

Remark 2.13. The weak imposition produces the same energy rate as the strong imposition with an additional damping term. A similar term will appear in the discrete approximation and stabilize it.

2.4. The continuous energy estimate. We have proved that if condition (2.28) and (2.29) required in Proposition 2.8 and 2.11 hold, the boundary condition (2.22) yield

$$(2.42) \quad \frac{d}{dt} \|\mathbf{v}\|_I^2 + 2\epsilon \|\nabla \mathbf{v}\|_I^2 \leq \oint g^T \Gamma g ds.$$

Time integration of (2.42) yields the final energy estimate

$$(2.43) \quad (\|\mathbf{v}\|_I^2)_{t=T} + 2\epsilon \int_0^T \|\nabla \mathbf{v}\|_I^2 dt \leq \|\mathbf{f}\|_I^2 + \int_0^T \oint g^T \Gamma g ds dt.$$

Remark 2.14. The relation (2.43) bounds the velocity field only. If only condition (2.34) holds, the estimate (2.43) holds with zero boundary data g . Note that no initial condition on the pressure is required.

3. APPLICATION OF THE GENERAL THEORY IN A FEW SPECIAL CASES

In this section we will consider a few commonly used boundary conditions, and relate them to the general theory developed above. Specific forms of the general boundary condition (2.22) can be derived by seeking matrices R and S such that

$$(3.1) \quad W^- - RW^+ = S \begin{bmatrix} BC_1 \\ BC_2 \end{bmatrix}.$$

In (3.1), BC_1 and BC_2 denotes the predetermined common boundary conditions and the matrix S (in general not the identity matrix) combines them.

Most boundary conditions required for an energy estimate are nonlinear, see Remark 2.7, while many commonly used boundary conditions are formulated in a linear way. The matrix S introduces the (sometimes) necessary nonlinearity and specific examples will be given below. Homogeneous boundary conditions are obtained by imposing (3.1) with zero right-hand side, while non-homogeneous conditions are obtained with non-zero data $S[BC_1, BC_2]^T = g$ on the right-hand side.

3.1. Solid wall and Dirichlet boundary conditions. For solid wall and Dirichlet conditions on the velocities [4, 24, 51], the form (2.22) derived using (3.1) becomes

$$(3.2) \quad W^- - RW^+ = S \begin{bmatrix} u_n \\ u_s \end{bmatrix}.$$

The solid wall and homogeneous Dirichlet conditions are obtained by imposing (3.2) with zero right-hand side, while non-homogeneous Dirichlet conditions are obtained with non-zero data on the right-hand side.

3.1.1. Boundary conditions in the rotated formulation. The sign of u_n changes the form of W^\pm in (3.2). Consider the inflow case for $u_n < 0$ and the variables in (2.14). The system (3.2) has the solution

$$(3.3) \quad R = \begin{bmatrix} 1 & 0 \\ 0 & -1 \end{bmatrix} \quad \text{and} \quad S = u_n \begin{bmatrix} 1 & 0 \\ 0 & 1 \end{bmatrix}.$$

We can prove

Proposition 3.1. The solid wall and homogeneous Dirichlet inflow boundary conditions (3.2) with R in (3.3) leads to an energy bound of the form (2.43) with zero boundary data.

Proof. From (2.14), (3.3) and a direct calculation, $\Lambda^+ + R^T \Lambda^- R = 0$ follows. Hence condition (2.34) required in Corollary 2.10 and 2.12 are satisfied. \square

Next, we examine the outflow case for $u_n > 0$ and consider (2.15). In these variables, the system defined by (3.2) has the solution

$$(3.4) \quad R = \begin{bmatrix} 1 & 0 \\ 0 & -1 \end{bmatrix} \quad \text{and} \quad S = u_n \begin{bmatrix} -1 & 0 \\ 0 & 1 \end{bmatrix}.$$

We can prove the following result, similar to Proposition 3.1.

Proposition 3.2. The solid wall and homogeneous Dirichlet outflow boundary conditions (3.2) with R in (3.4) leads to an energy bound of the form (2.43) with zero boundary data.

Proof. The proof of Proposition 3.2 is identical to the proof of Proposition 3.1. \square

Remark 3.3. Since condition (2.34) in Corollary 2.10 and 2.12, but not condition (2.28) in Proposition 2.8 holds, only estimates for zero right-hand sides in (3.2) are obtained.

3.1.2. Boundary conditions in the characteristic formulation. A unique expression (independent of the sign of u_n) for the in- and outgoing variables is given by (2.20). By solving for S and R in (3.2) we find

$$(3.5) \quad R = \begin{bmatrix} 0 & 1 \\ 1 & 0 \end{bmatrix} \quad \text{and} \quad S = \begin{bmatrix} d_1 & 0 \\ 0 & d_2 \end{bmatrix},$$

where $d_1 = \lambda_1 - \lambda_5 = -\sqrt{u_n^2 + 8}$ and $d_2 = \lambda_2 - \lambda_4 = -\sqrt{u_n^2 + 4}$.

We can prove

Proposition 3.4. The solid wall and homogeneous Dirichlet boundary conditions (3.2) with R in (3.5) leads to an energy bound of the form (2.43) with zero boundary data.

Proof. From (2.21) and (3.5), it follows that $\Lambda^+ + R^T \Lambda^- R = 0$, and hence condition (2.34) required in Corollary 2.10 and 2.12 holds. \square

Remark 3.3 holds also for the characteristic formulation.

3.2. Natural boundary conditions. Maybe the most established outflow boundary conditions for finite and spectral element approximations of the incompressible Navier-Stokes equations are the so-called natural (or "do-nothing") boundary conditions. These conditions appears automatically in the weak formulation after partial integration of the viscous terms and the pressure gradients [15, 14].

In the notation of this paper, the natural boundary conditions (hereafter denoted NBC) using the general form (3.1) becomes

$$(3.6) \quad W^- - RW^+ = S \begin{bmatrix} pn_x - \epsilon \partial_{\mathbf{n}} u \\ pn_y - \epsilon \partial_{\mathbf{n}} v \end{bmatrix}.$$

3.2.1. Boundary conditions in the rotated formulation. In the outflow formulation (2.15), the system defined by (3.6) has the solution

$$(3.7) \quad R = \begin{bmatrix} 0 & 0 \\ 0 & 0 \end{bmatrix} \quad \text{and} \quad S = \begin{bmatrix} n_x & n_y \\ n_y & -n_x \end{bmatrix},$$

which leads to the following Proposition.

Proposition 3.5. The NBC (3.6) with R in (3.7) leads to an energy bound of the form (2.43).

Proof. We find $\Lambda^+ + R^T \Lambda^- R = \Lambda^+ > 0$ and hence condition (2.28) required in Proposition 2.8 holds. \square

Remark 3.6. Since condition (2.28) in Proposition 2.8 holds, estimates for non-zero right-hand sides in (3.6) can be obtained.

3.2.2. Boundary conditions in the characteristic formulation. The in- and outgoing variables are given by (2.20). By solving for S and R in (3.6) we find

$$(3.8) \quad R = \begin{bmatrix} 0 & \lambda_1/\lambda_5 \\ \lambda_2/\lambda_4 & 0 \end{bmatrix} \quad \text{and} \quad S = \begin{bmatrix} d_1/\lambda_5 & 0 \\ 0 & d_2/\lambda_4 \end{bmatrix} \begin{bmatrix} n_x & n_y \\ -n_y & n_x \end{bmatrix}.$$

This lead to the following proposition.

Proposition 3.7. The NBC (3.6) with R in (3.8) leads to an energy bound of the form (2.43).

Proof. From (2.21) and (3.8), it follows that

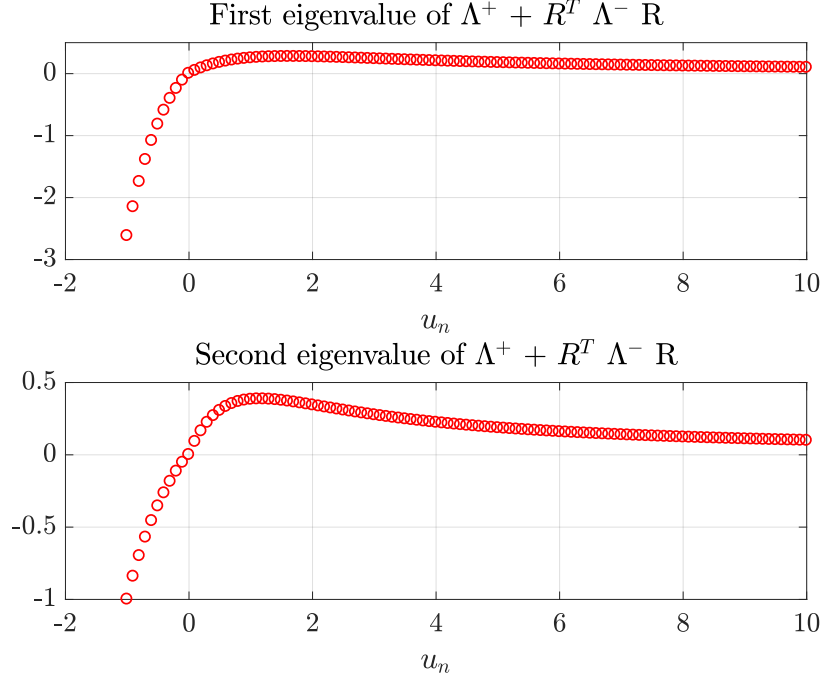
$$(3.9) \quad \Lambda^+ + R^T \Lambda^- R = \begin{bmatrix} \frac{\lambda_4}{1+\lambda_4^2} + \frac{\lambda_2^3}{\lambda_4^2(1+\lambda_2^2)} & 0 \\ 0 & \frac{\lambda_5}{2+\lambda_5^2} + \frac{\lambda_1^3}{\lambda_5^2(2+\lambda_1^2)} \end{bmatrix}.$$

Consider the first element in (3.9) and recall that $\lambda_2 + \lambda_4 = u_n > 0$. We find

$$\frac{\lambda_4}{1+\lambda_4^2} + \frac{\lambda_2^3}{\lambda_4^2(1+\lambda_2^2)} = \frac{\lambda_4^3(1+\lambda_2^2) + \lambda_2^3(1+\lambda_4^2)}{(1+\lambda_4^2)(1+\lambda_2^2)\lambda_4^2} = \frac{u_n((\lambda_4 - \lambda_2/2)^2 + 3\lambda_2^2/4 + \lambda_2^2\lambda_4^2)}{(1+\lambda_4^2)(1+\lambda_2^2)\lambda_4^2}$$

which is strictly positive. The second element in (3.9) is treated in the same way. \square

Remark 3.6 holds also for the characteristic formulation.

FIGURE 1. The two eigenvalues of (3.9) as a function of u_n .

3.3. Stabilized natural boundary conditions. The NBC discussed above become unstable when outflow conditions changes to inflow conditions at the boundary (u_n becomes negative), see Figure 1. Due to this effect, the so-called stabilized natural (or directional "do-nothing") boundary conditions for inflow boundaries has been derived [20, 3, 10].

The stabilized natural boundary conditions (hereafter denoted SNBC) using the general form (3.1) becomes

$$(3.10) \quad W^- - RW^+ = S \begin{bmatrix} \frac{1}{2}u_n u + pn_x - \epsilon \partial_{\mathbf{n}} u \\ \frac{1}{2}u_n v + pn_y - \epsilon \partial_{\mathbf{n}} v \end{bmatrix}.$$

3.3.1. Boundary conditions in the rotated formulation. In the inflow formulation (2.14), the system defined by (3.10) has the solution

$$(3.11) \quad R = \begin{bmatrix} -1 & 0 \\ 0 & 1 \end{bmatrix} \quad \text{and} \quad S = 2 \begin{bmatrix} n_x & n_y \\ -n_y & n_x \end{bmatrix},$$

which leads to the following Proposition.

Proposition 3.8. The SNBC (3.10) with R in (3.11) leads to an energy bound of the form (2.43) with zero boundary data.

Proof. We find $\Lambda^+ + R^T \Lambda^- R = \Lambda^+ = 0$ and hence condition (2.34) holds. \square

Remark 3.9. Since condition (2.34) in Corollary 2.10 and 2.12 holds, estimates for zero right-hand sides in (3.10) are obtained.

3.3.2. Boundary conditions in the characteristic formulation. The in- and outgoing variables are given by (2.20). By solving for S and R in (3.10) we find

$$(3.12) \quad R = - \begin{bmatrix} 0 & 1 \\ 1 & 0 \end{bmatrix} \quad \text{and} \quad S = 2 \begin{bmatrix} n_x & n_y \\ -n_y & n_x \end{bmatrix}.$$

This lead to the following proposition.

Proposition 3.10. The SNBC (3.10) with R in (3.12) leads to an energy bound of the form (2.43) with zero boundary data.

Proof. From (2.21) and (3.12), it follows that $\Lambda^+ + R^T \Lambda^- R = 0$ and consequently condition (2.34) holds. \square

Remark 3.9 holds also for the characteristic formulation.

3.4. External data requirements for the pressure. As stated in Remark 2.14, no initial condition for the pressure is required for the bound (2.43). Therefore, it is of interest to investigate if it is possible to derive matrices R in (2.22) which remove the pressure also from the boundary procedure and still obtain an energy estimate.

Consider boundary conditions (2.22) with the inflow rotated variables in (2.14). The set of matrices that removes the pressure from the boundary conditions have the form

$$(3.13) \quad R = \begin{bmatrix} 1 & r_{12} \\ 0 & r_{22} \end{bmatrix},$$

which yields $W^- - RW^+ = [u_n^2 - r_{12}\epsilon\partial_n u_s, u_n u_s - (1 + r_{22}\epsilon\partial_n u_s)]^T$. The coefficients r_{12} and r_{22} must be determined such that Proposition 2.8 and 2.11 (non-homogeneous case) or Corollary 2.10 and 2.12 (homogeneous case) hold. From (2.14) and (3.13), we find

$$(3.14) \quad \Lambda^+ + R^T \Lambda^- R = \frac{1}{u_n} \begin{bmatrix} 0 & r_{12} \\ r_{12} & -1 + r_{12}^2 + r_{22}^2 \end{bmatrix}.$$

By choosing

$$(3.15) \quad r_{12} = 0 \quad \text{and} \quad |r_{22}| \leq 1,$$

$\Lambda^+ + R^T \Lambda^- R$ has one zero and one non-negative eigenvalue and condition (2.34) holds. Similarly, in the outflow case, the same matrix as in (3.13) yields $W^- - RW^+ = [-u_n^2 + r_{12}\epsilon\partial_n u_s, -u_n u_s + (1 + r_{22}\epsilon\partial_n u_s)]^T$. As in the inflow case, condition (3.15) implies that (2.34) is satisfied.

Remark 3.11. Note that (3.15) includes the inflow R in (3.3) and the outflow R in (3.4) derived for the solid wall case in Section 3.1.1.

Consider the characteristic variables in (2.20). The set of matrices

$$(3.16) \quad R = \begin{bmatrix} r_{11} & 1 \\ r_{21} & 0 \end{bmatrix}$$

yields $W^- - RW^+ = [u_n(\lambda_1 - \lambda_5) - r_{11}(\lambda_4 u_s - \epsilon\partial_n u_s), u_n(\lambda_2 - r_{21}\lambda_4) + r_{21}\epsilon\partial_n u_s]^T$ which again does not involve the pressure. From (2.14) and (3.13), it follows that

$$(3.17) \quad \Lambda^+ + R^T \Lambda^- R = \begin{bmatrix} \frac{\lambda_4}{(1+\lambda_4^2)} + r_{21}^2 \frac{\lambda_2}{(1+\lambda_2^2)} + r_{11}^2 \frac{\lambda_1}{(2+\lambda_1^2)} & r_{11} \frac{\lambda_1}{(2+\lambda_1^2)} \\ r_{11} \frac{\lambda_1}{(2+\lambda_1^2)} & 0 \end{bmatrix}.$$

By choosing

$$(3.18) \quad r_{11} = 0 \quad \text{and} \quad |r_{21}| \leq 1,$$

$\Lambda^+ + R^T \Lambda^- R$ has one zero and one non-negative eigenvalue which implies that condition (2.34) holds.

Remark 3.12. Note that also condition (3.18) includes R in (3.5) derived for the solid wall case in Section 3.1.2.

We conclude that both formulations derived in this paper admit homogeneous energy bounding boundary conditions which do not include the pressure.

4. SIMILARITIES AND DIFFERENCES BETWEEN THE TWO FORMULATIONS

The two formulations require the same number of boundary conditions and they both lead to energy estimates. However, despite the similarities, there are differences, which will be discussed below.

4.1. The rotated boundary conditions. The form of the boundary conditions depends on whether there is an inflow or outflow situation at the boundary. This means that the boundary procedure must adapt to the time evolution of the solution.

Moreover, since the penalty matrix in (2.37) and conditions (2.28), (2.29) and (2.34) depend on the solution, care must be taken when the magnitude of the normal velocity assumes large or small values. From (2.14) and (2.15), it follows that $\Lambda^\pm = \pm I / |u_n|$. Hence, for $|u_n| \rightarrow 0$, $\Lambda^\pm \rightarrow \infty$, while for $|u_n| \rightarrow \infty$, $\Lambda^\pm \rightarrow 0$. This indicates that this formulation might be problematic for $|u_n|$ small.

Proposition 4.1. The boundary conditions (2.22) in the rotated formulation bounds (2.16) if $R^T R \neq I$ for $|u_n| \geq \delta > 0$. The bound is obtained for both the strong and the weak imposition.

Proof. Consider the diagonal matrices in (2.14) and (2.15). The lower bound in (2.29) becomes $\Gamma \geq [I + R(I_2 - R^T R)^{-1} R^T] / |u_n|$. Hence, conditions (2.28) and (2.29) in Proposition 2.8 and 2.11 are both satisfied. \square

For a weak imposition in the solid wall case, the possible problem with a vanishing normal velocity is removed. To clarify, consider the general penalty term in (2.36) with Σ from (2.34) and $\mathbf{g} = 0$. In the inflow case, we get

$$\Sigma(W^- - RW^+) = (H^-)^T \Lambda^- S \begin{bmatrix} u_n \\ u_s \end{bmatrix} = (H^-)^T \begin{bmatrix} u_n \\ u_s \end{bmatrix}, \quad \text{where} \quad H^- = \begin{bmatrix} 0 & 0 & 1 & -1 & 0 \\ 0 & 0 & 0 & 0 & 1 \end{bmatrix}^T,$$

while in the outflow case

$$\Sigma(W^- - RW^+) = (H^-)^T \Lambda^- S \begin{bmatrix} u_n \\ u_s \end{bmatrix} = (H^-)^T \begin{bmatrix} u_n \\ -u_s \end{bmatrix}, \quad \text{where} \quad H^- = \begin{bmatrix} u_n & 0 & 1 & -1 & 0 \\ 0 & u_n & 0 & 0 & 1 \end{bmatrix}^T.$$

In both cases, H^- is bounded as $u_n \rightarrow 0^\pm$. Hence, the singularities that would seemingly occur for vanishing u_n are eliminated.

4.2. The characteristic boundary conditions. The in- and outgoing characteristic boundary conditions have a fixed form independent of the solution. Furthermore, all the eigenvalues in (2.17) and the corresponding eigenvectors in (2.18) remain bounded for all values of $|u_n|$. In particular, condition (2.29) is automatically satisfied if (2.28) holds, which proves the following relaxed version of Proposition 2.8

Proposition 4.2. The boundary conditions (2.22) in the characteristic formulation bounds (2.16) if $\Lambda^+ + R^T \Lambda^- R > 0$ holds. The bound holds for both the strong and the weak imposition.

Also, in the solid wall case, all the matrices involved in condition (3.5) are bounded when $u_n \rightarrow 0^\pm$, which leads to a well-defined formulation.

Remark 4.3. The comparison in Section 4.1 and 4.2 shows that the characteristic formulation is more suitable than the rotated formulation. It is well-defined for all flow cases and have the same form for all values of u_n . In the remaining numerical part of the paper, we will limit ourselves to the characteristic formulation of boundary conditions.

Remark 4.4. The analysis in this paper is for clarity and brevity made for the two-dimensional (2D) case. In three dimensions (3D), the same principal analysis can be made. The changes are purely technical and amounts to replacing the 2D integration-by-parts results with the 3D corresponding ones (line integrals will turn into surface integrals). The key properties and definitions remain the same, but for a slightly larger system of equations. In the semi-discrete and fully discrete case discussed below, this technical change is mimicked by adding one more dimension in the tensor (Kronecker) products. As in the continuous case, the key properties and definitions remain the same, but for a larger system of equations

5. THE SEMI-DISCRETE APPROXIMATION

To discretize the system (2.36) in space, we consider an approximation on SBP-SAT form. In order to make the paper self-contained, we provide a brief introduction to the SBP-SAT approximation and recommend [52, 48, 31, 13] for a complete description. We present the technique for schemes in tensor product form, but the derivation is valid for all approximations on SBP-SAT form. To derive a semi-discrete energy estimate, we will mimic the analysis of the continuous case above.

Consider a two-dimensional Cartesian grid of $N \times M$ points with coordinates (x_i, y_j) . The west, east, south and north boundaries are indicated by $b \in \{W, E, S, N\}$ and the normals at each boundary by $\mathbf{n}^b = (n_x^b, n_y^b)$, see Figure 2.

The discrete approximation of a variable $v = v(x, y)$ is a vector of length $N \times M$ arranged as $\mathbf{v} = (v_{11}, \dots, v_{1M}, v_{21}, \dots, v_{2M}, \dots, v_{N1}, \dots, v_{NM})^T$, where $v_{ij} \approx v(x_i, y_j)$.

The SBP approximation of the spatial partial derivatives of v are given by

$$D_x \mathbf{v} = (P_x^{-1} Q_x \otimes I_M) \mathbf{v} \approx \frac{\partial \mathbf{v}}{\partial x} \quad \text{and} \quad D_y \mathbf{v} = (I_N \otimes P_y^{-1} Q_y) \mathbf{v} \approx \frac{\partial \mathbf{v}}{\partial y},$$

where I_d is the identity matrix of dimension d and \otimes denotes the Kronecker product [22]. The matrices $P_{x,y}$ are diagonal, positive definite and such that the product $(P_x \otimes P_y)$ forms a quadrature rule which defines a discrete L^2 norm $\|\mathbf{v}\|_{P_x \otimes P_y}^2 =$

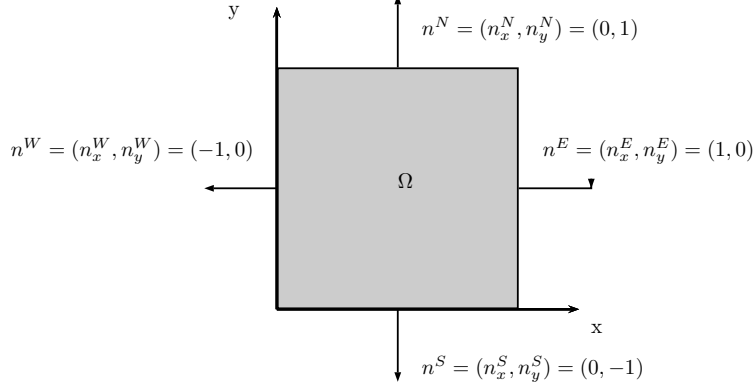


FIGURE 2. Two-dimensional domain showing the outward pointing normals.

$\mathbf{v}^T(P_x \otimes P_y)\mathbf{v}$. The operators $Q_{x,y}$ are almost skew-symmetric matrices satisfying the SBP property

$$(5.1) \quad Q_x + Q_x^T = -E_0 + E_N, \quad Q_y + Q_y^T = -E_0 + E_M,$$

where $E_0 = \text{diag}(1, 0, \dots, 0)$ and $E_{N,M} = \text{diag}(0, \dots, 0, 1)$, with the appropriate dimensions. The matrix $D(\mathbf{a})$ has the components of the vector \mathbf{a} injected on the diagonal.

Remark 5.1. The form of the projection matrices E_0 and $E_{N,M}$ implies that the first and last grid points are located precisely at the boundaries. This choice avoids certain stability problems [41]. Note also that nowhere in the description above is the accuracy of the discrete derivative operators specified, which allows for arbitrary high order accurate schemes.

5.1. The semi-discrete formulation. Consider the time-dependent vector $\mathbf{V} = (\mathbf{u}(t), \mathbf{v}(t), \mathbf{p}(t))^T$ and the discrete version of (2.2)

$$(5.2) \quad \mathbf{A} = \begin{bmatrix} D(\mathbf{u}) & \mathbf{0} & I_{NM} \\ \mathbf{0} & D(\mathbf{u}) & \mathbf{0} \\ I_{NM} & \mathbf{0} & \mathbf{0} \end{bmatrix}, \mathbf{B} = \begin{bmatrix} D(\mathbf{v}) & \mathbf{0} & \mathbf{0} \\ \mathbf{0} & D(\mathbf{v}) & I_{NM} \\ \mathbf{0} & I_{NM} & \mathbf{0} \end{bmatrix}, \tilde{I}_3 = \begin{bmatrix} I_{NM} & \mathbf{0} & \mathbf{0} \\ \mathbf{0} & I_{NM} & \mathbf{0} \\ \mathbf{0} & \mathbf{0} & \mathbf{0} \end{bmatrix}.$$

Here, \mathbf{A}, \mathbf{B} and \tilde{I}_3 are $3NM \times 3NM$ matrices while $\mathbf{0}$ is a $NM \times NM$ matrix of zeros.

With this notation, the semi-discrete SBP-SAT approximation of (2.36) becomes

$$(5.3) \quad \tilde{I}_3 \mathbf{V}_t + \tilde{D}_x \mathbf{V} + \tilde{D}_y \mathbf{V} - \epsilon \left[(\tilde{I} \otimes D_x)^2 + (\tilde{I} \otimes D_y)^2 \right] \mathbf{V} = \text{Pen}_{\text{BT}},$$

where the skew-symmetric splitting (2.4) is approximated by the operators

$$(5.4) \quad \tilde{D}_x = \frac{1}{2}(I_3 \otimes D_x)\mathbf{A} + \frac{1}{2}\mathbf{A}(I_3 \otimes D_x), \quad \tilde{D}_y = \frac{1}{2}(I_3 \otimes D_y)\mathbf{B} + \frac{1}{2}\mathbf{B}(I_3 \otimes D_y).$$

In (5.3), Pen_{BT} is the discrete version of the lifting operator in (2.36). It can be decomposed into the sum of four terms corresponding to each boundary of the

square domain, namely $\text{Pen}_{\text{BT}} = \text{Pen}_{\text{BT}}^W + \text{Pen}_{\text{BT}}^E + \text{Pen}_{\text{BT}}^S + \text{Pen}_{\text{BT}}^N$, where

$$(5.5) \quad \begin{aligned} \text{Pen}_{\text{BT}}^W &= (I_3 \otimes (P_x^{-1} E_0 \otimes I_M)) \boldsymbol{\Sigma}^W (\mathbf{H}^W \mathbf{V} - G^W), \\ \text{Pen}_{\text{BT}}^E &= (I_3 \otimes (P_x^{-1} E_N \otimes I_M)) \boldsymbol{\Sigma}^E (\mathbf{H}^E \mathbf{V} - G^E), \\ \text{Pen}_{\text{BT}}^S &= (I_3 \otimes (I_N \otimes P_y^{-1} E_0)) \boldsymbol{\Sigma}^S (\mathbf{H}^S \mathbf{V} - G^S), \\ \text{Pen}_{\text{BT}}^N &= (I_3 \otimes (I_N \otimes P_y^{-1} E_M)) \boldsymbol{\Sigma}^N (\mathbf{H}^N \mathbf{V} - G^N). \end{aligned}$$

The matrices $\mathbf{H}^{W,E,S,N}$ are the discrete boundary operators related to H in (2.6) and $G^{W,E,S,N}$ are vectors containing the boundary data at the appropriate boundary points. Finally, $\boldsymbol{\Sigma}^{W,E,S,N}$ are penalty matrices to be determined.

5.2. The semi-discrete energy estimate. The discrete energy method applied to (5.3) (multiplying the equation from the left by $\mathbf{V}^T(I_3 \otimes P_x \otimes P_y)$ and adding its transpose) and the SBP properties in (5.1) yield

$$(5.6) \quad \frac{d}{dt} \|\mathbf{V}\|_{\tilde{P}}^2 + \mathbf{Diss} = \mathbf{BT} + \mathbf{V}^T(I_3 \otimes P_x \otimes P_y) \text{Pen}_{\text{BT}} + (\mathbf{V}^T(I_3 \otimes P_x \otimes P_y) \text{Pen}_{\text{BT}})^T,$$

where $\mathbf{Diss} = 2\epsilon(\|(I_3 \otimes D_x)\mathbf{V}\|_{\tilde{P}}^2 + \|(I_3 \otimes D_y)\mathbf{V}\|_{\tilde{P}}^2)$. As in (2.8), $\|\mathbf{V}\|_{\tilde{P}}^2 = \mathbf{V}^T(\tilde{I} \otimes P_x \otimes P_y)\mathbf{V}$ defines a discrete semi-norm such that (5.6) represents the discrete energy rate of the velocity field $(\mathbf{u}, \mathbf{v})^T$. The notation \mathbf{BT} stands for the discrete boundary term corresponding to (2.9) in the continuous case. It contains the four contributions from each boundary of the domain, i.e. $\mathbf{BT} = \mathbf{BT}^W + \mathbf{BT}^E + \mathbf{BT}^S + \mathbf{BT}^N$, where

$$(5.7) \quad \begin{aligned} \mathbf{BT}^W &= -\mathbf{V}^T(I_3 \otimes -E_0 \otimes P_y) \mathbf{A} \mathbf{V} + 2\epsilon \mathbf{V}^T(I_3 \otimes -E_0 \otimes P_y)(\tilde{I} \otimes D_x) \mathbf{V}, \\ \mathbf{BT}^E &= -\mathbf{V}^T(I_3 \otimes E_N \otimes P_y) \mathbf{A} \mathbf{V} + 2\epsilon \mathbf{V}^T(I_3 \otimes E_N \otimes P_y)(\tilde{I} \otimes D_x) \mathbf{V}, \\ \mathbf{BT}^S &= -\mathbf{V}^T(I_3 \otimes P_x \otimes -E_0) \mathbf{B} \mathbf{V} + 2\epsilon \mathbf{V}^T(I_3 \otimes P_x \otimes -E_0)(\tilde{I} \otimes D_y) \mathbf{V}, \\ \mathbf{BT}^N &= -\mathbf{V}^T(I_3 \otimes P_x \otimes E_M) \mathbf{B} \mathbf{V} + 2\epsilon \mathbf{V}^T(I_3 \otimes P_x \otimes E_M)(\tilde{I} \otimes D_y) \mathbf{V}. \end{aligned}$$

Following the continuous analysis, we will rewrite each term in \mathbf{BT} as a quadratic form similar to (2.11). First, we project \mathbf{V} onto the boundaries by $\mathbf{V}^b = B^b \mathbf{V}$, where

$$(5.8) \quad B^b = \begin{cases} E_0 \otimes I_M & \text{on the west boundary,} \\ E_N \otimes I_M & \text{on the east boundary,} \\ I_N \otimes E_0 & \text{on the south boundary,} \\ I_N \otimes E_M & \text{on the north boundary} \end{cases}$$

and $b \in W, E, S, N$. Next, the discrete analogue of (2.10) is

$$(5.9) \quad \mathbf{w}^b = \begin{bmatrix} \mathbf{u}_{n^b} \\ \mathbf{u}_{s^b} \\ \mathbf{p}^b \\ \epsilon D_{\mathbf{n}} \mathbf{u}_{n^b} \\ \epsilon D_{\mathbf{n}} \mathbf{u}_{s^b} \end{bmatrix} = \mathbf{T}^b \mathbf{V}^b, \quad \mathbf{T}^b = \begin{bmatrix} n_x^b I_{NM} & n_y^b I_{NM} & 0 \\ -n_y^b I_{NM} & n_x^b I_{NM} & 0 \\ 0 & 0 & I_{NM} \\ \epsilon D_{\mathbf{n}^b} n_x^b & \epsilon D_{\mathbf{n}^b} n_y^b & 0 \\ -\epsilon D_{\mathbf{n}^b} n_y^b & \epsilon D_{\mathbf{n}^b} n_x^b & 0 \end{bmatrix},$$

where $D_{\mathbf{n}^b} = n_x^b D_x + n_y^b D_y$ approximates the normal derivative.

By applying (5.9) and rearranging, each term in (5.7) can be written

$$(5.10) \quad \mathbf{B}\mathbf{T}^b = -(\mathbf{w}^b)^T (I_5 \otimes P^b) \underbrace{\begin{bmatrix} D(\mathbf{u}_{n^b}) & 0 & I_{NM} & -I_{NM} & 0 \\ 0 & D(\mathbf{u}_{n^b}) & 0 & 0 & -I_{NM} \\ I_{NM} & 0 & 0 & 0 & 0 \\ -I_{NM} & 0 & 0 & 0 & 0 \\ 0 & -I_{NM} & 0 & 0 & 0 \end{bmatrix}}_{\mathbf{A}_{\mathbf{n}}^b} \mathbf{w}^b.$$

Here, P^b is an operator which approximates a line-integral along boundary b , namely

$$(5.11) \quad P^b = \begin{cases} E_0 \otimes P_y & \text{on the west boundary,} \\ E_N \otimes P_y & \text{on the east boundary,} \\ P_x \otimes E_0 & \text{on the south boundary,} \\ P_x \otimes E_M & \text{on the north boundary.} \end{cases}$$

Remark 5.2. All matrices in (5.10) are diagonal, which implies that we are dealing with NM (the total number of grid points) decoupled quadratic forms, each associated to a grid point. The operator P^b projects the variables onto boundary b and removes the contributions from the internal grid points. Hence, the number of non-zero terms in (5.10) is equal to the number of boundary points.

Remark 5.2 implies that (5.10) can be rewritten as

$$(5.12) \quad \mathbf{B}\mathbf{T}^b = -(\mathbf{w}^b)^T (I_5 \otimes P^b) \mathbf{A}_{\mathbf{n}^b} \mathbf{w}^b = \sum_{l \in b} -(\mathbf{w}_l)^T P_{ll}^b (\mathbf{A}_{\mathbf{n}^b})_l \mathbf{w}_l,$$

where $l \in b$ indicates the set of points belonging to the boundary $b \in W, E, S, N$. In (5.12), $\mathbf{w}_l = (\mathbf{w}^b)_l$ is the variable at a specific boundary point, P_{ll}^b is the corresponding diagonal element in P^b and $(\mathbf{A}_{\mathbf{n}^b})_l$ is the pointwise version of $\mathbf{A}_{\mathbf{n}}$ in (2.11).

5.3. The discrete boundary conditions. We derive the discrete boundary condition by replicating step-by-step the continuous procedure in 2.2, but limit ourselves to the weak implementation of the characteristic variable formulation.

5.3.1. The discrete diagonalization. Since all the matrices $(\mathbf{A}_{\mathbf{n}^b})_l$ in (5.12) have exactly the same structure as $\mathbf{A}_{\mathbf{n}}$ in (2.11), they can be diagonalized by the eigenvalue decomposition already derived in Section 2.2.2. The negative and positive eigenvalues from each $(\mathbf{A}_{\mathbf{n}^b})_l$ define the vectors $\boldsymbol{\lambda}_{1,2}^b$ and $\boldsymbol{\lambda}_{4,5}^b$, respectively. Their components are the pointwise version of (2.17) on boundary b . The block-diagonal discrete version of (2.21) is

$$(5.13) \quad \boldsymbol{\Lambda}^{-,b} = \begin{bmatrix} D(\boldsymbol{\lambda}_1^b/(2 + (\boldsymbol{\lambda}_1^b)^2)) & \mathbf{0} \\ \mathbf{0} & D(\boldsymbol{\lambda}_2^b/(1 + (\boldsymbol{\lambda}_2^b)^2)) \end{bmatrix},$$

$$(5.14) \quad \boldsymbol{\Lambda}^{+,b} = \begin{bmatrix} D(\boldsymbol{\lambda}_4^b/(1 + (\boldsymbol{\lambda}_4^b)^2)) & \mathbf{0} \\ \mathbf{0} & D(\boldsymbol{\lambda}_5^b/(2 + (\boldsymbol{\lambda}_5^b)^2)) \end{bmatrix},$$

where the division should be interpreted elementwise. Furthermore, let

$$(5.15) \quad (\mathbf{X}^{-,b})^T = \begin{bmatrix} D(\lambda_1^b) & \mathbf{0} & I_{NM} & -I_{NM} & \mathbf{0} \\ \mathbf{0} & D(\lambda_2^b) & \mathbf{0} & \mathbf{0} & -I_{NM} \end{bmatrix},$$

$$(5.16) \quad (\mathbf{X}^{+,b})^T = \begin{bmatrix} \mathbf{0} & D(\lambda_4^b) & \mathbf{0} & \mathbf{0} & -I_{NM} \\ D(\lambda_5^b) & \mathbf{0} & I_{NM} & -I_{NM} & \mathbf{0} \end{bmatrix}$$

be the block-diagonal version of (2.27). We define the discrete in- and outgoing characteristic variables as $\mathbf{W}^{-,b} = (\mathbf{X}^{-,b})^T \mathbf{w}^b$ and $\mathbf{W}^{+,b} = (\mathbf{X}^{+,b})^T \mathbf{w}^b$, respectively. With this notation, (5.12) becomes

$$(5.17) \quad \mathbf{B}\mathbf{T}^b = - \begin{bmatrix} \mathbf{W}^{+,b} \\ \mathbf{W}^{-,b} \end{bmatrix}^T (I_4 \otimes P^b) \begin{bmatrix} \mathbf{\Lambda}^{+,b} & \mathbf{0} \\ \mathbf{0} & \mathbf{\Lambda}^{-,b} \end{bmatrix} \begin{bmatrix} \mathbf{W}^{+,b} \\ \mathbf{W}^{-,b} \end{bmatrix}$$

5.3.2. The discrete form of the boundary conditions. Recall that the continuous boundary conditions were imposed in the form (2.22) and, hence, we want to construct boundary operators \mathbf{H}^b in (5.5) in a similar way. Consider (5.15) and (5.16) and define the boundary operators

$$(5.18) \quad \mathbf{H}^{+,b} = (\mathbf{X}^{+,b})^T \mathbf{T}^b (I_3 \otimes B^b), \quad \mathbf{H}^{-,b} = (\mathbf{X}^{-,b})^T \mathbf{T}^b (I_3 \otimes B^b),$$

with B^b as in (5.8) and \mathbf{T}^b as in (5.9). These operators project \mathbf{V} onto the boundary b and transform it to the discrete in- and outgoing characteristic variables, $\mathbf{W}^{+,b}$ and $\mathbf{W}^{-,b}$ in (5.17). Hence, the discrete version of (2.23) on the boundary b becomes

$$(5.19) \quad \mathbf{H}^b \mathbf{V} = \mathbf{H}^{-,b} \mathbf{V} - \mathbf{R} \mathbf{H}^{+,b} \mathbf{V} = \mathbf{W}^{-,b} - \mathbf{R} \mathbf{W}^{+,b}$$

where $\mathbf{R} = [R \otimes I_{NM}]$ is the block-diagonal version of R in (2.22). In particular, the discrete boundary condition at a solid wall (3.2) is obtained by choosing R as in (3.5).

5.4. Stability of the discrete weak implementation. By considering (5.17) and using (5.19) in (5.5), the discrete energy rate (5.6) can be rewritten as

$$(5.20) \quad \frac{d}{dt} \|\mathbf{V}\|_{\tilde{P}}^2 + \mathbf{Diss} = - \sum_{e \in \{W, E, S, N\}} \begin{bmatrix} \mathbf{W}^{+,b} \\ \mathbf{W}^{-,b} \end{bmatrix}^T (I_4 \otimes P^b) \begin{bmatrix} \mathbf{\Lambda}^{+,b} & \mathbf{0} \\ \mathbf{0} & \mathbf{\Lambda}^{-,b} \end{bmatrix} \begin{bmatrix} \mathbf{W}^{+,b} \\ \mathbf{W}^{-,b} \end{bmatrix} + \mathbf{V}^T (I_3 \otimes P^b) \mathbf{\Sigma}^b (\mathbf{W}^{-,b} - \mathbf{R} \mathbf{W}^{+,b} - G^b) + \mathbf{V}^T (I_3 \otimes P^b) \mathbf{\Sigma}^b (\mathbf{W}^{-,b} - \mathbf{R} \mathbf{W}^{+,b} - G^b)^T$$

which is the discrete analogue of (2.38). We can now follow the procedure in the continuous analysis and use similar conditions to get a bound. We choose

$$(5.21) \quad \mathbf{\Sigma}^b = (\mathbf{H}^{-,b})^T \mathbf{\Lambda}^{-,b},$$

as penalty matrix with $\mathbf{\Lambda}^{-,b}$ given in (5.13), which leads to

$$\frac{d}{dt} \|\mathbf{V}\|_{\tilde{P}}^2 + \mathbf{Diss} = - \sum_{e \in \{W, E, S, N\}} \begin{bmatrix} \mathbf{W}^{+,b} \\ \mathbf{W}^{-,b} \\ G^b \end{bmatrix}^T (I_6 \otimes P^b) \begin{bmatrix} \mathbf{\Lambda}^{+,b} & \mathbf{R}^T \mathbf{\Lambda}^{-,b} & \mathbf{0} \\ \mathbf{\Lambda}^{-,b} \mathbf{R} & -\mathbf{\Lambda}^{-,b} & \mathbf{\Lambda}^{-,b} \\ \mathbf{0} & \mathbf{\Lambda}^{-,b} & \mathbf{0} \end{bmatrix} \begin{bmatrix} \mathbf{W}^{+,b} \\ \mathbf{W}^{-,b} \\ G^b \end{bmatrix},$$

which corresponds to (2.39). By introducing a positive semi-definite matrix $\mathbf{\Gamma}^b$ and adopting the splitting in (2.40), the bound for the discrete energy rate with

non-zero data G^b becomes

$$(5.22) \quad \frac{d}{dt} \|\mathbf{V}\|_{\tilde{P}}^2 + 2\epsilon \left(\|(\tilde{I} \otimes D_x)\mathbf{V}\|_{\tilde{P}}^2 + \|(\tilde{I} \otimes D_y)\mathbf{V}\|_{\tilde{P}}^2 \right) \leq \sum_{b \in \{W, E, S, N\}} (G^b)^T (I_2 \otimes P^b) \mathbf{\Gamma}^b G^b.$$

For the characteristic boundary conditions, all the diagonal elements in (5.13) and (5.14) remain bounded for all possible values of the components \mathbf{u}_n^b . The conditions on $\mathbf{\Lambda}^{\pm, b}$, \mathbf{R} for which a bounded $\mathbf{\Gamma}^b$ exists and (5.22) constitutes a bound are given in

Proposition 5.3. The semi-discrete approximation (5.3) of (2.36) with penalty matrix (5.21) and boundary operators (5.18)-(5.19) leads to stability if

$$(5.23) \quad \mathbf{\Lambda}^{+, b} + \mathbf{R}^T \mathbf{\Lambda}^{-, b} \mathbf{R} > 0.$$

Proof. See the proof of Proposition 2.11 and 4.2. \square

In the homogeneous cases, the proof of Corollary 2.12 proves

Corollary 5.4. The semi-discrete approximation (5.3) of (2.36) with homogeneous boundary conditions and penalty matrix (5.21) leads to stability if

$$(5.24) \quad \mathbf{\Lambda}^{+, b} + \mathbf{R}^T \mathbf{\Lambda}^{-, b} \mathbf{R} \geq 0.$$

Remark 5.5. We have for simplicity and ease of presentation exemplified the theoretical development with an SBP-SAT scheme in tensor product form on a 2D rectangular domain. A similar derivation can be done on curvilinear domains that can be divided into patches, where each patch can be smoothly mapped to a square (2D) or a cube (3D). For fully unstructured SBP-SAT methods, not on tensor product form, even more general domains can be handled.

6. THE FULLY DISCRETE FORMULATION

To advance the divergence relation in time, we use the SBP-SAT technique also in time on (5.3) and impose the initial condition (2.7) weakly. To make the analysis self-contained, we shortly introduce this procedure and recommend [38, 29, 2] for more details.

Consider a two-dimensional spatial grid with NM points and L time levels. The fully-discrete approximation of a variable $v = v(t, x, y)$ is a vector of length $LN M$ arranged as follows

$$\mathbf{v} = \begin{bmatrix} \vdots \\ [\mathbf{v}]_k \\ \vdots \end{bmatrix}, [\mathbf{v}]_k = \begin{bmatrix} \vdots \\ [\mathbf{v}]_{ki} \\ \vdots \end{bmatrix}, [\mathbf{v}]_{ki} = \begin{bmatrix} \vdots \\ v_{kij} \\ \vdots \end{bmatrix}, \quad \text{where } v_{kij} \approx v(t_k, x_i, y_j).$$

Each vector component \mathbf{v}_k has length NM and represents the discrete variable on the spatial domain at time level k . The SBP approximation of the time derivative is

$$(D_t \otimes I_N \otimes I_M) \mathbf{v} = (P_t^{-1} Q_t \otimes I_N \otimes I_M) \mathbf{v} \approx \frac{\partial v}{\partial t},$$

where P_t and Q_t satisfy the same properties as the spatial operators.

6.1. The fully-discrete formulation. Consider the fully-discrete variable $\mathbf{V} = [\mathbf{V}_1, \dots, \mathbf{V}_k, \dots, \mathbf{V}_L]^T$, where each $\mathbf{V}_k = (\mathbf{u}_k, \mathbf{v}_k, \mathbf{p}_k)^T$ represents the variables on the whole spatial domain at the k -th time level. The SBP-SAT approximation of (2.36) including a weak imposition of the boundary and initial conditions can be written

$$(6.1) \quad (D_t \otimes \tilde{I}_3) \mathbf{V} + \mathbf{F}(\mathbf{V}) \mathbf{V} = \mathbf{Pen}_{\text{BT}} + \mathbf{Pen}_{\text{Time}}.$$

Here, $\mathbf{F} = \text{blockdiag}(F(\mathbf{V}_0), \dots, F(\mathbf{V}_L))$ where the blocks are the nonlinear spatial differential operators given by

$$(6.2) \quad F(\mathbf{V}_k) = (\tilde{D}_x)_k + (\tilde{D}_y)_k - \epsilon \left[(\tilde{I} \otimes D_x)^2 + (\tilde{I} \otimes D_y)^2 \right], \quad k = 0, \dots, L.$$

The nonlinearity in (6.2) is due to the form of $(\tilde{D}_x)_k$ and $(\tilde{D}_y)_k$ given in (5.4).

In (6.1), \mathbf{Pen}_{BT} is a vector of penalty terms for weakly imposing the boundary conditions at each time level, i.e.

$$(6.3) \quad \mathbf{Pen}_{\text{BT}} = [(\text{Pen}_{\text{BT}})_0, \dots, (\text{Pen}_{\text{BT}})_k, \dots, (\text{Pen}_{\text{BT}})_L]^T$$

where each $(\text{Pen}_{\text{BT}})_k$ is the sum of the four boundary penalties given in (5.5). Finally, $\mathbf{Pen}_{\text{Time}}$ is the penalty term for weakly imposing the initial condition given by

$$(6.4) \quad \mathbf{Pen}_{\text{Time}} = \sigma_t (P_t^{-1} E_0 \otimes \tilde{I} \otimes I_N \otimes I_M) (\mathbf{V} - \mathbf{f}),$$

where \mathbf{f} is a vector of the same length as \mathbf{V} containing the initial data at $k = 0$.

Remark 6.1. Note that no initial condition is imposed on the pressure in (6.4). This is in line with the continuous analysis in Section 2.4.

6.2. The fully discrete energy estimate. Consider the diagonal matrix $P = (P_t \otimes I_3 \otimes P_x \otimes P_y)$ and let $\|\mathbf{v}\|_P^2 = \mathbf{v}^T P \mathbf{v}$ be a discrete L^2 norm with respect to time and space. We can prove

Proposition 6.2. The approximation (6.1) of (2.36), with spatial penalty terms (6.3) satisfying the assumptions of Proposition 5.3 (or Corollary 5.4), is stable with the temporal penalty term (6.4) and $\sigma_t = -1$.

Proof. We apply the discrete energy method to (6.1) (multiplying the equation from the left by $V^T P$ and adding its transpose) to get

$$(6.5) \quad \mathbf{V}^T P \left[(D_t + D_t^T) \otimes \tilde{I}_3 \right] \mathbf{V} + \mathbf{V}^T \left(P \mathbf{F}(\mathbf{V}) + \mathbf{F}^T P \right) \mathbf{V} = \\ + \mathbf{V}^T P \mathbf{Pen}_{\text{BT}} + (\mathbf{V}^T P \mathbf{Pen}_{\text{BT}})^T + 2\sigma_t \mathbf{V}_0^T (\tilde{I} \otimes P_x \otimes P_y) (\mathbf{V}_0 - \mathbf{f}),$$

with \tilde{I}_3 from (5.2). By applying the SBP property (5.1) to the temporal differential operator, the first term on the left-hand side of (6.5) can be rewritten as

$$(6.6) \quad \mathbf{V}^T P \left[(D_t + D_t^T) \otimes \tilde{I}_3 \right] \mathbf{V} = \mathbf{V}^T \left(B_t \otimes \tilde{I} \otimes P_x \otimes P_y \right) \mathbf{V} = \|\mathbf{V}_L\|_P^2 - \|\mathbf{V}_0\|_P^2,$$

where $B_t = D(-1, 0, \dots, 0, 1)$ and $\|\mathbf{V}_k\|_P^2$, $k = 0, L$, is the discrete semi-norm at the first and last time level with respect to space.

From (6.2) and the SBP property (5.1) applied to the spatial differential operator, the second term in (6.5) can be expanded into

$$(6.7) \quad \mathbf{V}^T (P\mathbf{F}(\mathbf{V}) + \mathbf{F}(\mathbf{V})^T P) \mathbf{V} = 2\epsilon \left(\|(P_t \otimes \tilde{I} \otimes D_x)\mathbf{V}\|_P^2 + \|(P_t \otimes \tilde{I} \otimes D_y)\mathbf{V}\|_P^2 \right) - \mathbf{B}\mathbf{T}.$$

Here, $\mathbf{B}\mathbf{T}$ is the vector $\mathbf{B}\mathbf{T} = [(\mathbf{B}\mathbf{T})_0, \dots, (\mathbf{B}\mathbf{T})_k, \dots, (\mathbf{B}\mathbf{T})_L]^T$, where each $\mathbf{B}\mathbf{T}_k$ represents the boundary term on the right-hand side of (5.6) at time level k . It can be written as the sum of the four contributions coming from each boundary as in (5.7). With conditions (5.23) (or (5.24) in the homogeneous cases) satisfied at each time level, (5.22) follows and consequently

$$(6.8) \quad \mathbf{B}\mathbf{T} + \mathbf{V}^T P \text{Pen}_{\mathbf{B}\mathbf{T}} + (\mathbf{V}^T P \text{Pen}_{\mathbf{B}\mathbf{T}})^T \leq \sum_{e \in \{W, E, S, N\}} (\mathbf{G}^b)^T (P_t \otimes I_2 \otimes P^b) \mathbf{\Gamma}^b \mathbf{G}^b.$$

In (6.8), $\mathbf{G}^b = [G_0^b, \dots, G_k^b, \dots, G_L^b]^T$ contains the boundary data G_k^b on boundary b at time level k , P^b is from (5.11) and $\mathbf{\Gamma}^b = \text{blockdiag}(\Gamma_0^b, \dots, \Gamma_L^b)$, where each Γ_k^b is a bounded positive definite matrix.

Remark 6.3. The estimate (6.8) follows directly from the semi-discrete stability.

By considering (6.6), (6.7) and (6.8), relation (6.5) becomes

$$(6.9) \quad \|\mathbf{V}_L\|_P^2 \leq \sum_{e \in \{W, E, S, N\}} (\mathbf{G}^b)^T (P_t \otimes I_3 \otimes P^b) \mathbf{\Gamma}^b \mathbf{G}^b + \|\mathbf{V}_0\|_P^2 + 2\sigma_t \mathbf{V}_0^T (\tilde{I} \otimes P_x \otimes P_y) (\mathbf{V}_0 - \mathbf{f}).$$

Next, we add and subtract $\|\mathbf{f}\|_P^2$ to (6.9) which leads to

$$(6.10) \quad \|\mathbf{V}_L\|_P^2 \leq \|\mathbf{f}\|_P^2 + \sum_{e \in \{W, E, S, N\}} (\mathbf{G}^b)^T (P_t \otimes I_3 \otimes P^b) \mathbf{\Gamma}^b \mathbf{G}^b + \begin{bmatrix} \mathbf{V}_0 \\ \mathbf{f} \end{bmatrix}^T \begin{bmatrix} 1 + 2\sigma_t & -\sigma_t \\ -\sigma_t & -1 \end{bmatrix} \otimes (\tilde{I} \otimes P_x \otimes P_y) \begin{bmatrix} \mathbf{V}_0 \\ \mathbf{f} \end{bmatrix}.$$

The last term in (6.10) is negative semi-definite if and only if $\sigma_t = -1$, which yields

$$(6.11) \quad \|\mathbf{V}_L\|_P^2 \leq \|\mathbf{f}\|_P^2 + \sum_{e \in \{W, E, S, N\}} (\mathbf{G}^b)^T (P_t \otimes I_3 \otimes P^b) \mathbf{\Gamma}^b \mathbf{G}^b - \|\mathbf{V}_0 - \mathbf{f}\|_P^2,$$

and we have a bound. \square

Remark 6.4. Note that (6.11) is the fully discrete version of the continuous estimate (2.43) and the semi-discrete estimate (5.22) with an additional damping term due to the weak imposition of the initial condition. As in the continuous and semi-discrete case, it is a bound for the numerical velocity field only.

Remark 6.5. The SBP-SAT strategy in time leads to *i)* high order accuracy, *ii)* unconditional stability and *iii)* it preserves nonlinear semi-discrete stability. In this paper we specifically took advantage of *iii)* when we went from semi-discrete stability directly to fully discrete stability, see Remark 6.3. Regarding efficiency, a large system of nonlinear set of equations must be solved, which is a disadvantage. However, the multi-block/stage formulation of the method in finite difference form discussed in [29] reduces the block sizes to a minimum and transforms the global method to a time-marching one. If one uses the spectral element operators based

on Gauss–Lobatto quadrature as SBP operators to discretise time, the block size can be even further reduced. For these operators, it was shown in [2] that the SBP-SAT formulation is equivalent to the Lobatto IIIC type of classical Runge–Kutta methods.

7. CONCLUSIONS

An investigation on the initial boundary value problem for the incompressible nonlinear Navier-Stokes equations have been presented. The velocity-divergence formulation of the problem was chosen to ensure a divergence free solution without additional artificial procedures. The boundary conditions were obtained by considering two different techniques to diagonalize the boundary terms. In particular, a set of non-singular rotations and a standard eigenvalue decomposition lead to the rotated and characteristic formulation, respectively.

The two forms of boundary conditions were strongly and weakly imposed and was adapted to different situations at far field and solid boundaries. Integration in time and space together with the implementations of the derived boundary conditions lead to energy estimates. In particular: solid wall, Dirichlet, natural and stabilized natural boundary conditions were investigated and related to the new formulations. It was observed that the resulting boundary conditions were often nonlinear. It was also shown that external pressure data was not required in order to obtain an estimate. A comparison between the two forms of conditions revealed that the characteristic formulation is more suitable than the rotated formulation since it is always well-defined and have the same form at outflow and inflow boundaries.

The numerical approximation of the governing equations using differential operators on SBP form and SAT penalty techniques for imposing the initial and boundary conditions was performed by mimicking the analysis of the continuous problem in a step-by-step fashion. The discrete analysis was carried out for an approximation on tensor product form, but is valid for all types of approximations on SBP-SAT form. The resulting scheme was shown to be stable if the same conditions and penalty terms as in the continuous case were used. Both semi-discrete and fully discrete estimates were obtained.

This paper can be summarised as follows. We derive energy bounding boundary conditions for the nonlinear incompressible Navier-Stokes equations by using the energy method. The continuous derivation is the target and roadmap for the discrete analysis. By mimicking the continuous analysis, the semi-discrete approximation is proven stable using SBP-SAT in space. Finally, the semi-discrete stability results leads directly to fully discrete stability, by using SBP-SAT also in time.

REFERENCES

1. Douglas N Arnold, Franco Brezzi, Bernardo Cockburn, and L Donatella Marini, *Unified analysis of discontinuous Galerkin methods for elliptic problems*, SIAM Journal on Numerical Analysis **39** (2002), no. 5, 1749–1779.
2. Pieter D. Boom and David.W Zingg, *High-order implicit time-marching methods based on generalized summation-by-parts operators*, SIAM Journal on Scientific Computing **37** (2015), no. 6, A2682–A2709.
3. Malte Braack and Piotr B Mucha, *Directional do-nothing condition for the Navier–Stokes equations*, Journal of Computational Mathematics **32** (2014), no. 5, 507–5211.
4. Arnim Brüger, Bertil Gustafsson, Per Lötstedt, and Jonas Nilsson, *High order accurate solution of the incompressible Navier–Stokes equations*, Journal of Computational Physics **203** (2005), no. 1, 49–71.

5. Mark H Carpenter, Travis C Fisher, Eric J Nielsen, and Steven H Frankel, *Entropy stable spectral collocation schemes for the Navier–Stokes equations: Discontinuous interfaces*, SIAM Journal on Scientific Computing **36** (2014), no. 5, B835–B867.
6. Mark H Carpenter and David Gottlieb, *Spectral methods on arbitrary grids.*, Journal of Computational Physics **129** (1996), 74–86.
7. Mark H Carpenter, David Gottlieb, and Saul Abarbanel, *Time-stable boundary conditions for finite-difference schemes solving hyperbolic systems: Methodology and application to high-order compact schemes*, Journal of Computational Physics **111** (1994), no. 2, 220–236.
8. P Castonguay, DM Williams, PE Vincent, and A Jameson, *Energy stable flux reconstruction schemes for advection–diffusion problems*, Computer Methods in Applied Mechanics and Engineering **267** (2013), 400–417.
9. D.C. Del Rey Fernández, J.E. Hicken, and D.W. Zingg, *Simultaneous approximation terms for multi-dimensional summation-by-parts operators*, Accepted in Journal of Scientific Computing (2017).
10. S. Dong, G.E. Karniadakis, and C. Chrysosostomidis, *A robust and accurate outflow boundary condition for incompressible flow simulations on severely truncated unbounded domains*, Journal of Computational Physics **261** (2014), 83–105.
11. Travis C Fisher, Mark H Carpenter, Jan Nordström, Nail K Yamaleev, and Charles Swanson, *Discretely conservative finite-difference formulations for nonlinear conservation laws in split form: Theory and boundary conditions*, Journal of Computational Physics **234** (2013), 353–375.
12. Luca Formaggia, Jean-Frédéric Gerbeau, Fabio Nobile, and Alfio Quarteroni, *On the coupling of 3D and 1D Navier–Stokes equations for flow problems in compliant vessels*, Computer Methods in Applied Mechanics and Engineering **191** (2001), no. 6, 561–582.
13. Gregor J Gassner, *A skew-symmetric discontinuous Galerkin spectral element discretization and its relation to SBP–SAT finite difference methods*, SIAM Journal on Scientific Computing **35** (2013), no. 3, A1233–A1253.
14. Roland Glowinski, *Finite element methods for Navier–Stokes equations*, Annual Review of Fluid Mechanics **24** (1992), 167–204.
15. P. M. Gresho, *Some current cfd issues relevant to the incompressible Navier–Stokes equations*, Computer Methods in Applied Mechanics and Engineering **87** (1991), 201–252.
16. Bertil Gustafsson and Jonas Nilsson, *Boundary conditions and estimates for the steady Stokes equations on staggered grids*, Journal of Scientific Computing **15** (2000), no. 1, 29–59.
17. Albert Gyr and Franz-S Rys, *Diffusion and transport of pollutants in atmospheric mesoscale flow fields*, vol. 1, Springer Science & Business Media, 2013.
18. William D Henshaw, *A fourth-order accurate method for the incompressible Navier–Stokes equations on overlapping grids*, Journal of Computational Physics **113** (1994), no. 1, 13–25.
19. Jan S Hesthaven and David Gottlieb, *A stable penalty method for the compressible Navier–Stokes equations: I. open boundary conditions*, SIAM Journal on Scientific Computing **17** (1996), no. 3, 579–612.
20. J.G. Heywood, R. Rannacher, and S. Turek, *Artificial boundaries and flux and pressure conditions for the incompressible Navier–Stokes equations*, International Journal for Numerical Methods in Fluids **22** (1996), 325–352.
21. Charles Hirsch, *Numerical computation of internal and external flows: The fundamentals of computational fluid dynamics*, Butterworth-Heinemann, 2007.
22. Roger A Horn and Charles R Johnson, *Matrix analysis*, Cambridge university press, 2012.
23. Ht T Huynh, *A flux reconstruction approach to high-order schemes including discontinuous Galerkin methods*, 18th AIAA Computational Fluid Dynamics Conference, 2007, p. 4079.
24. Christer Johansson, *Boundary conditions for open boundaries for the incompressible Navier–Stokes equation*, Journal of Computational Physics **105** (1993), no. 2, 233–251.
25. John Kim and Parviz Moin, *Application of a fractional-step method to the incompressible Navier–Stokes equations*, Journal of Computational Physics **59** (1985), no. 2, 308–323.
26. Sinisa Krajnovic and Lars Davidson, *Large-eddy simulation of the flow around simplified car model*, SAE paper (2004), 01–0227.
27. Heinz-Otto Kreiss and Jens Lorenz, *Initial-boundary value problems and the Navier–Stokes equations*, vol. 47, SIAM, 1989.
28. Wendy Kress and Jonas Nilsson, *Boundary conditions and estimates for the linearized Navier–Stokes equations on staggered grids*, Computers & Fluids **32** (2003), no. 8, 1093–1112.

29. Tomas Lundquist and Jan Nordström, *The SBP-SAT technique for initial value problems*, Journal of Computational Physics **270** (2014), 86–104.
30. John Marshall, Alistair Adcroft, Chris Hill, Lev Perelman, and Curt Heisey, *A finite-volume, incompressible Navier-Stokes model for studies of the ocean on parallel computers*, Journal of Geophysical Research: Oceans **102** (1997), no. C3, 5753–5766.
31. Ken Mattsson and Jan Nordström, *Summation by parts operators for finite difference approximations of second derivatives*, Journal of Computational Physics **199** (2004), no. 2, 503–540.
32. Jan Nordström, *The use of characteristic boundary conditions for the Navier–Stokes equations*, Computers & Fluids **24** (1995), no. 5, 609–623.
33. ———, *Conservative finite difference formulations, variable coefficients, energy estimates and artificial dissipation*, Journal of Scientific Computing **29** (2006), no. 3, 375–404.
34. ———, *A Roadmap to Well Posed and Stable Problems in Computational Physics*, Journal of Scientific Computing **71** (2017), no. 1, 365–385.
35. Jan Nordström, Sofia Eriksson, and Peter Eliasson, *Weak and strong wall boundary procedures and convergence to steady-state of the Navier–Stokes equations*, Journal of Computational Physics **231** (2012), no. 14, 4867–4884.
36. Jan Nordström, Karl Forsberg, Carl Adamsson, and Peter Eliasson, *Finite volume methods, unstructured meshes and strict stability for hyperbolic problems*, Applied Numerical Mathematics **45** (2003), no. 4, 453–473.
37. Jan Nordström, Jing Gong, Edwin van der Weide, and Magnus Svärd, *A stable and conservative high order multi-block method for the compressible Navier–Stokes equations*, Journal of Computational Physics **228** (2009), no. 24, 9020–9035.
38. Jan Nordström and Tomas Lundquist, *Summation-by-parts in time*, Journal of Computational Physics **251** (2013), 487–499.
39. Jan Nordström, Ken Mattsson, and Charles Swanson, *Boundary conditions for a divergence free velocity–pressure formulation of the Navier–Stokes equations*, Journal of Computational Physics **225** (2007), no. 1, 874–890.
40. Jan Nordström, Niklas Nordin, and Dan Henningson, *The fringe region technique and the Fourier method used in the direct numerical simulation of spatially evolving viscous flows*, SIAM Journal on Scientific Computing **20** (1999), no. 4, 1365–1393.
41. Jan Nordström and Andrea Ruggiu, *On conservation and stability properties for summation-by-parts schemes*, Journal of Computational Physics **344** (2017), 451–464.
42. Jan Nordström and Magnus Svärd, *Well-posed boundary conditions for the Navier–Stokes equations*, SIAM Journal on Numerical Analysis **43** (2005), no. 3, 1231–1255.
43. S Ognier, D Iya-Sou, C Fourmond, and S Cavadias, *Analysis of mechanisms at the plasma–liquid interface in a gas–liquid discharge reactor used for treatment of polluted water*, Plasma Chemistry and Plasma Processing **29** (2009), no. 4, 261–273.
44. N Anders Petersson, *Stability of pressure boundary conditions for Stokes and Navier–Stokes equations*, Journal of Computational Physics **172** (2001), no. 1, 40–70.
45. Hendrik Ranocha, Philipp Öffner, and Thomas Sonar, *Summation-by-parts operators for correction procedure via reconstruction*, Journal of Computational Physics **311** (2016), 299–328.
46. Alan Shapiro, *The use of an exact solution of the Navier-Stokes equations in a validation test of a three-dimensional nonhydrostatic numerical model*, Monthly Weather Review **121** (1993), no. 8, 2420–2425.
47. Chiara Sargentone, Cristina La Cognata, and Jan Nordström, *A new high order energy and enstrophy conserving Arakawa-like Jacobian differential operator*, Journal of Computational Physics **301** (2015), 167–177.
48. B. Strand, *Summation by parts for finite difference approximations for d/dx* , Journal of Computational Physics **110** (1994), 47–67.
49. John C Strikwerda and Young S Lee, *The accuracy of the fractional step method*, SIAM Journal on Numerical Analysis **37** (1999), no. 1, 37–47.
50. Magnus Svärd, Mark H Carpenter, and Jan Nordström, *A stable high-order finite difference scheme for the compressible Navier–Stokes equations, far-field boundary conditions*, Journal of Computational Physics **225** (2007), no. 1, 1020–1038.
51. Magnus Svärd and Jan Nordström, *A stable high-order finite difference scheme for the compressible Navier–Stokes equations: no-slip wall boundary conditions*, Journal of Computational Physics **227** (2008), no. 10, 4805–4824.

52. ———, *Review of summation-by-parts schemes for initial-boundary-value problems*, Journal of Computational Physics **268** (2014), 17–38.
53. Charles A. Taylor, Thomas J.R. Hughes, and Christopher K. Zarins, *Finite element modeling of blood flow in arteries*, Computer Methods in Applied Mechanics and Engineering **158** (1998), 155–196.
54. Geoffrey K Vallis, *Atmospheric and oceanic fluid dynamics: fundamentals and large-scale circulation*, Cambridge University Press, 2006.
55. Niklas Wintermeyer, Andrew R. Winters, Gregor J. Gassner, and David A. Kopriva, *An entropy stable nodal discontinuous Galerkin method for the two dimensional shallow water equations on unstructured curvilinear meshes with discontinuous bathymetry*, Journal of Computational Physics **340** (2017), 200 – 242.
56. J. Yan, J. Crean, and J.E Hicken, *Interior penalties for summation-by-parts discretizations of linear second-order differential equations*, Accepted in Journal of Scientific Computing (2017).

DEPARTMENT OF MATHEMATICS, COMPUTATIONAL MATHEMATICS, LINKÖPING UNIVERSITY, LINKÖPING, SE-581 83, SWEDEN

E-mail address: `jan.nordstrom@liu.se`

DEPARTMENT OF MATHEMATICS, COMPUTATIONAL MATHEMATICS, LINKÖPING UNIVERSITY, LINKÖPING, SE-581 83, SWEDEN

E-mail address: `cristina.la.cognata@liu.se`